Reinforcement of Polyimine Covalent Adaptable Networks with Mechanically Interlocked Derivatives of SWNTs

Ion Isasti, Silvia Miranda, David M. Jiménez, Sylwia Parzyszek, Natalia Martín Sabanés, Henrik Pedersen, Emilio M. Pérez

Reinforcement of polyimine covalent adaptable networks with mechanically interlocked derivatives of SWNTs.

*Ion Isasti, Silvia Miranda, David M. Jiménez, Sylwia Parzyszek, Natalia Martín Sabanés Henrik Pedersen and Emilio M. Pérez**

I. Isasti, Dr. S. Miranda, D. M. Jiménez, S. Parzyszek, Dr. N. Martín Sabanés and Prof. E. M. Pérez
IMDEA Nanociencia, Faraday 9, Ciudad Universitaria de Canto Blanco, E28049 Madrid, Spain
E-mail: emilio.perez@imdea.org

Dr. H. Pedersen
Nanocore ApS, Gothersgade 21, DK-1123, Copenhagen K, Denmark

Keywords: covalent adaptable networks, single-walled carbon nanotubes, composites, mechanically interlocked molecules, recyclable

There is an urgent need for new approaches to reduce the environmental impact of plastics. One approach is to enhance recyclability. Covalent adaptable networks (CANs), where crosslinks are chemically reversible, offer an attractive alternative to thermoset materials. Another option is to strengthen polymers using nanofillers, to reduce the amount of material needed. In this regard, single-walled carbon nanotubes (SWNTs) are excellent candidates as fillers due to their extreme strength-to-weight ratio and dimensionality. Here, SWNTs functionalized as mechanically-interlocked derivatives (MINTs) are shown to significantly improve the mechanical properties of polyimine (PI) CANs, with close to optimal efficiency. Enhancements in both stiffness and ultimate strength, approaching 100% load transfer considering the SWNT loading, are observed for PI MINT, while composites made with pristine SWNTs exhibit poor improvement. The PI MINT CANs can be recycled both thermally and chemically without compromising their mechanical properties. Finally, prototype carbon fiber PI MINT laminar composites are also fabricated and characterized, demonstrating a significant increase in their mechanical properties.

1. Introduction

Plastics are inexpensive materials that can readily be shaped into a variety of products that find use in a broad range of applications. Based on these intrinsic properties, the use of plastics has quickly generalised around the globe. This has had a tremendous positive impact in our quality of life, yet it now poses a serious environmental problem.[1] Current levels of usage and disposal of plastics are unsustainable even in the short term.[2] While we find definitive, long-term solutions to this problem, we need to develop technologies that can reduce the amount of plastics significantly and help mitigate it as much as possible. One possible approach is to reinforce plastics with adequate fillers, so that a smaller amount of composite can serve the

same purpose as a larger amount of non-reinforced plastic. Another approach is to facilitate recycling of polymers,[3] for example by reducing the use of thermosets and intensifying the use of thermoplastics, which can be melted and reshaped for further use.[4] In this sense, reinforcement of thermoplastics is often needed,[5] as otherwise their mechanical properties are significantly inferior to those of thermosets.

A very attractive solution to this tug-of-war between mechanical performance and recyclability are covalent adaptable networks (CANs),[6] which are polymer networks built out of dynamic covalent bonds.[7] CANs combine the strength provided by the chemical crosslinks with the adaptability provided by dynamic chemistry. A couple of selected recent examples will help locate the state-of-the-art in this field. For example, a supramolecular version of CANs leading to mechanically strong networks that can be recycled at room temperature was recently described.[8] Their design is based on imine bond formation for the building of the CAN and secondary H-bonding for further crosslinking. Very recently, the combined power of the chemistry of disulfide exchange and transesterification was exploited by Zhang and co-workers to build self-repairing IR transmitting CANs.[9]

Single-walled carbon nanotubes (SWNTs) are cylindrical nanostructures made entirely of sp^2-bound carbon atoms arranged in a hexagonal pattern. This chemical structure makes CNTs extremely strong, with a Young‘s modulus of 1-5 TPa (calculated)[10] and most likely around 1 TPa as experimentally measured.[11] This is about five times stiffer than structural steel, while also being approximately four times less dense. These exceptional properties are in principle ideal for SWNTs to be used as polymer fillers, which are often brittle and/or deform easily. Consequently, blending polymers with SWNT fillers has emerged as a vibrant area of research in composite materials.[12] Nevertheless, the observed enhancements in mechanical properties of SWNT-polymer composites often fall significantly short of theoretical predictions, primarily due to challenges in individualizing SWNTs and achieving effective load transfer from the polymer matrix to the nanotubes.

The extraordinary potential of the combination of CANs and SWNTs has only recently started to be investigated, mostly with the aim of making use of the electronic properties of the SWNTs,[13] but it is largely unexplored with regards to providing mechanically superior and recyclable composites.[14]

In the last ten years, our group,[15] and others,[16] have described the synthesis of mechanically interlocked derivatives of SWNTs (MINTs).[17] MINTs are rotaxane-type derivatives in which macrocyclic molecules wrap around SWNTs. We have provided proof-of-principle studies that show that wrapping the SWNTs within a mechanically interlocked layer of macrocycles[18, 19] or polymer[20] is a valid strategy to enhance the performance of SWNTs as fillers.[21] The concept is simple: by surrounding the SWNT with organic material, we simultaneously prevent/decrease aggregation and provide sites of interaction with the polymer, which enhance load transfer.

Here, we show that MINTs can be used to reinforce polyimine (PI) CANs very efficiently (improvement of 77% in Young's modulus and 100% tensile strength at 1% w/w SWNT loading). The MINT-PI composite can be melted and reshaped, ensuring full recyclability. Moreover, we demonstrate the proof-of-principle use of MINT-PI as binder in single ply carbon-fiber composites, in which we measure a remarkable improvement of 66% in Young's modulus 73% in tensile strength.

2. Results and discussion

2.1. Molecular design and synthesis of MINTs

We have previously shown that wrapping SWNTs within a molecular layer of macrocyclic structures facilitates the dispersion of the carbonaceous filler and improves the polymer-SWNT interaction.[18, 19] With regards to the latter, we showed that the interaction depends on the chemical nature of the polymer matrix and the macrocycles following standard supramolecular chemistry principles.[19] Taking this into account, and since our objective was to reinforce a PI

matrix, we designed a U-shaped macrocycle precursor featuring two pyrene units for association with the SWNTs. The recognition units are decorated by long alkyl chains terminated in alkenes for ring-closing metathesis. The aromatic spacer between the two pyrene units is functionalized with an amide link to a bifurcated bisamine fragment. This structure is easily synthesized from commercially available precursors using standard chemical procedures (see the Supporting Information) and can participate in the PI structure via amine exchange. The Boc-protected precursor to the U-shaped molecule was closed around SWNTs to form MINTs using ring-closing metathesis, and characterized after standard purification procedures by TGA, Raman, and AFM, which proved the interlocked nature of the macrocycles around the SWNT (see the Supporting Information). Subsequent Boc deprotection under thermal conditions (220 ºC, 2h, loss of Boc group monitored by TGA) yielded the free diamine MINTs (daMINT in **Figure 1a**).[17] As a control sample, we also synthesized another MINT based on the same design principles, but lacking the diamine functionalities, and therefore unable to participate in the PI structure (ctrlMINT in **Figure 1a**). The synthesis of ctrlMINT and its characterization have been reported elsewhere.[20]

On the other hand, the PI CAN features terephthaldeyde (TPA) and diethylene triamine (DETA) as linear growth monomers, with tris(2-aminoethyl)amine (TREN) as crosslinker, used in a 1.00/0.30/0.47 TPA/DETA/TREN molar ratio a combination that was recently described by Yu and cols. (**Figure 1b**).[22] Upon mixing with the daMINT filler, it is expected that it can participate in the imine exchange reaction, therefore connecting the matrix and the filler through the mechanical bond, so that the daMINTs form an integral part of the CAN (**Figure 1c**) and the load transfer is maximized.[20] This hypothesis was corroborated in preliminary experiments testing the reactivity of the U-shape with TPA, which showed changes in the FTIR spectra compatible with formation of the imine (see the Supporting Information).

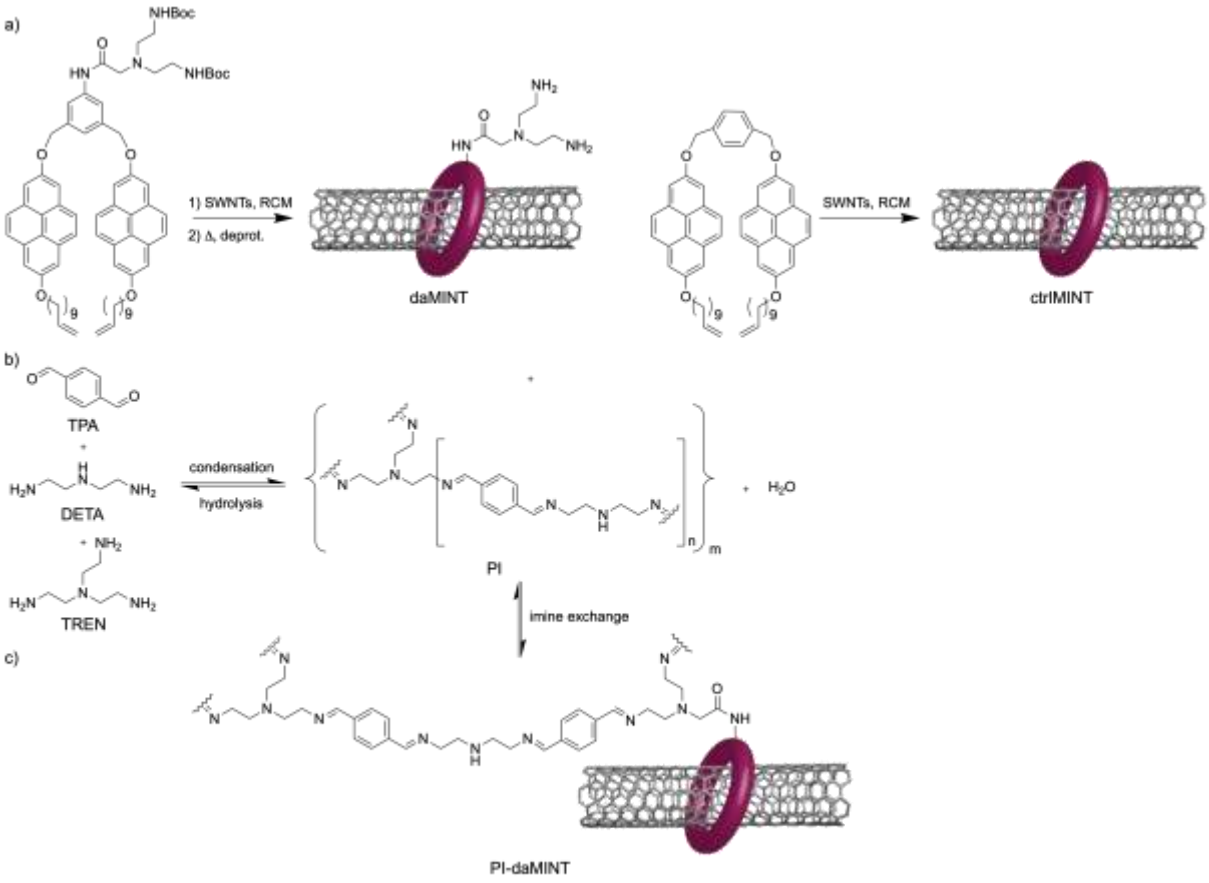

Figure 1. a) Chemical structure of the Boc-protected U-shape macrocyclic precursor, synthesis of daMINT and ctrlMINTs, and idealized representation of the structure of the MINTs (note that 1+1 macrocyclization is also possible). b) Chemical structures of the dialdehyde (TPA) and diamine (DETA), and the triamine (TREN) cross-linker used for growth of the PI network and simplified chemical structure of the PI CAN. c) Simplified chemical structure of the PI-daMINT CAN.

2.2. Fabrication of PI composites with SWNT and MINT fillers:

To ensure crosslinking of the daMINT material and facilitate dispersion, we first mixed TPA and daMINTs (or ctrlMINTs or SWNTs) in a planetary ball-mill reactor and milled the mixture for 10 min at 250 rpm (see Experimental Section for details). Then DETA and TREN were added dropwise while mixing manually, and the mixture was further milled for 10 more minutes

at 250 rpm. The resulting paste was removed from the reactor and mixed manually before returning it to the ball-mill for a last milling process of 20 min, also at 25 rpm. The paste obtained after this procedure was placed a hot-press and cured for 1 h at 75 ºC, 1 h at 85ºC and 3 h at 105 ºC all at 80 bars pressure, obtaining films of ≈0.2 mm thickness, which were used for characterization.

2.3 Mechanical characterization

The mechanical properties of the pure PI and its composites with pristine SWNTs, daMINTs and ctrlMINTs, all at 1% w/w loading of SWNTs, were characterized in tensile tests. To this end, films of each sample as obtained after the hot-press procedure were cut into dog-bone probes, and at three (or more) of these were subjected to mechanical testing. The data are shown in **Figure 2d** and **e**, and can be summarized as follows. The PI CAN shows a Young's modulus (YM) of 1.81 ± 0.04 GPa and ultimate tensile strength (TS) of 34 ± 9 MPa (black Figure 2). These values are comparable to those reported for a structurally similar PI CAN,[23] and confirm that our samples are satisfactorily cross-linked. The PI-SWNT is barely reinforced by addition of the SWNTs, showing YM = 1.8 ± 0.2 GPa and TS = 37 ± 3 MPa, which we attribute to the poor dispersion of the pristine SWNTs in the PI matrix, which is evident in optical microscopy of a PI-SWNT film (**Figure 2b**). In comparison, the PI-daMINT sample shows much better dispersion and forms microscopically more uniform films (**Figure 2c**), and consequently displays remarkable reinforcement, with YM = 3.2 ±0.2 GPa and TS = 68 ± 9 MPa, an increase by 77% and 100%, respectively. In turn, the PI-ctrlMINT sample showed YM = 2.4 ±0.2 GPa and TS = 48 ± 4 MPa. With these data, we can conclude that the derivatization of SWNTs as MINTs helps the reinforcement significantly, but optimal performance requires that the rings can crosslink chemically with the PI CAN structure.

Assuming a YM of 1TPa and TS of 100 GPa for the SWNT fillers, for the PI-daMINT samples we calculate a load transfer of ≈120 % with regards to YM and ≈30% for TS using the rule of

mixtures for randomly oriented fibers (see the Supporting Information for details). The first one is obviously an overestimation, due to either experimental error or underestimation of the YM of SWNTs.[10] In any case, these values reflect the success of the daMINT structural design, achieving very close to optimal use of the extraordinary properties of the SWNT, at least in terms of stiffness.[24] For comparison, for the PI-SWNT sample we calculate a very poor load transfer of ≈ 3% both in terms of YM and TS.

To investigate the mechanism of reinforcement further, we performed Raman spectroscopy (λ_{exc} = 785 nm) on the PI-SWNT and PI-daMINT composites at 0%, 1%, 2% strain, and after fracture. The results are summarized in Figure S3 and show that the shifts of the G and 2D bands are quantitatively larger in the case of the PI-daMINT samples. This effect is particularly noticeable in the shift of the 2D band. These changes in the Raman spectra are a spectroscopic consequence of a more effective load transfer to the SWNTs.[25]

Finally, we also investigated the fracture regions under scanning electron microscopy (SEM). The results are shown in Figure 2 f-h. The fracture area of the PI-SWNT sample shows the SWNTs in random orientations, indicating that their initial arrangement in the composite has not been modified during the stress test. In contrast, in the PI-daMINT sample we clearly observe an effect of orientation of the SWNTs along the direction of the applied stress, indicative of a much better load transfer.

Remarkably, the mechanical properties of the PI-daMINT composite are not altered after recycling. The samples used for the thermal tests were melted and hot-pressed into new dog-bones that afforded the following data YM = 3.13 ± 0.06 GPa and TS = 60 ± 3 MPa. We repeated the thermal recycling process up to three times, without detriment to the mechanical properties of the PI-daMINT composites (see the Supporting Information). The neat PI and PI SWNTs samples also afforded similar data after recycling, with YM = 1.6 ± 0.2 GPa and TS = 33 ± 6 MPa and YM = 1.7 ±0.2 GPa and TS = 40 ± 2 MPa, respectively.

As an alternative recycling process, we also investigated the complete depolymerization of the PI by chemical treatment with excess propylamine. The propylamine solution was poured into a container, repolymerized and processed after evaporation of the propylamine. The mechanical test on this sample afforded YM = 3.12 GPa and TS = 59 MPa (see the Supporting Information), demonstrating the feasibility of chemical recycling of the PI-daMINT composite.

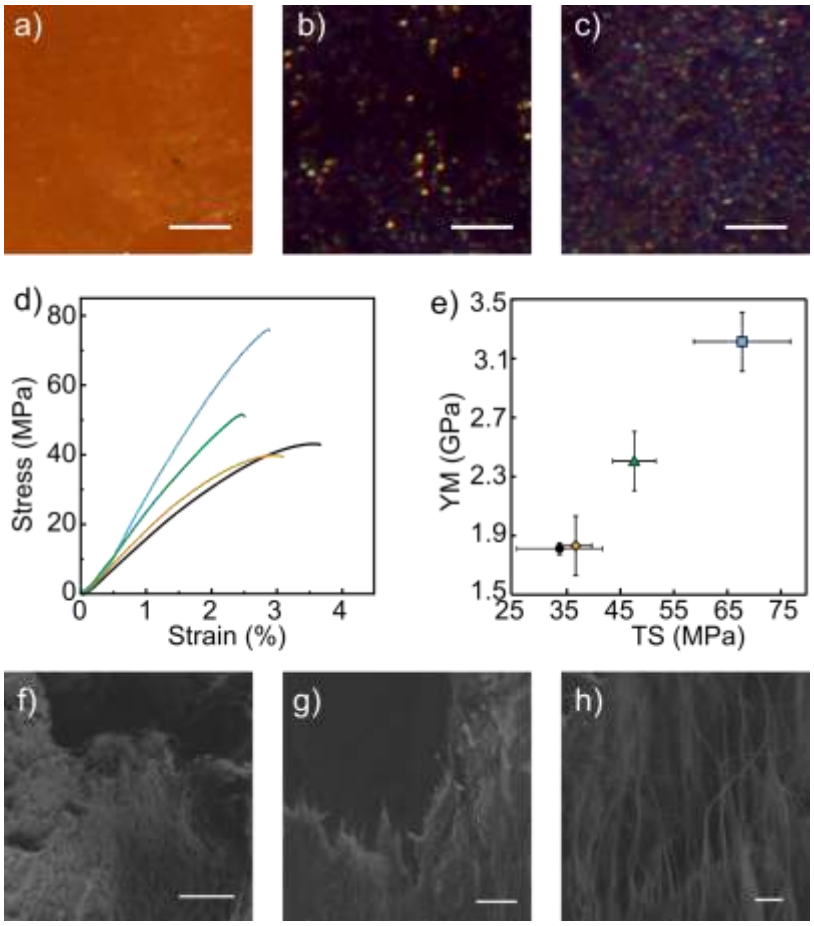

Figure 2. Optical micrographs of a) PI, b) PI-SWNTs and c) PI-daMINTs. Scale bars are 5 µm. d) Representative stress-strain curves for PI (black), PI-SWNTs (orange), PI-ctrlMINT (green) and PI-daMINTs (blue). e) YM vs TS plot for the data obtained from the average data of three stress-strain curves recorded for PI (black circle), PI-SWNTs (orange rhomboid), PI-ctrlMINT (green triangle) and PI-daMINTs (blue square), the error bars represent the standard deviation. SEM micrographs of the fracture areas of f) PI-SWNTs, g and h) PI-daMINTs. Scale bars are 2 µm for f and g, and 300 nm for h.

With these extremely encouraging results, we decided to test the limits of the daMINT approach by making 5% w/w SWNT composites. For the PI-SWNT sample we obtained YM = 2.5 ± 0.3 GPa and TS = 42 ± 4 MPa, while for the PI-daMINT sample, we measured YM = 3.3 ± 0.2 GPa and TS = 62 ± 5 MPa. While the daMINT filler keeps being significantly more effective than the pristine SWNTs, the load transfer decreased to ≈ 27% for the YM, indicating that the increase in loading is compensated for by a decrease in the quality of the dispersion. Considering this, we decided to continue our study with the 1% w/w samples only.

To gain insight into dynamic mechanical behavior and viscoelastic properties of our composites, we performed dynamic mechanical analysis (DMA). The results are summarized in **Figure 3**. For the neat PI CAN we obtain a storage modulus of 1.17 GPa at 25 ºC, which increases only very slightly to 1.24 GPa for PI-SWNTs and soars to 2.22 GPa for PI-daMINT (Figure 3a), an improvement > 85 %, in very good agreement with the tensile test data. Reflecting this enhancement in mechanical properties, a very significant increase in temperature of glass transition (Tg) is also apparent from Figure 3b, from 81 ºC for PI, which remains approximately equal for PI SWNTs (Tg = 82 ºC), to 92 ºC in the case of PI-daMINTs.

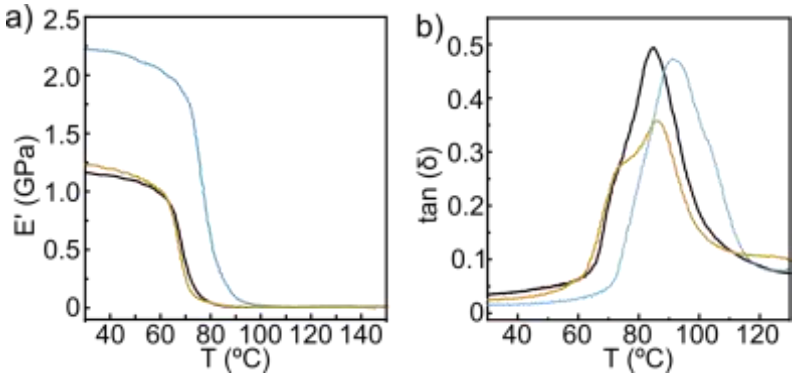

Figure 3. DMA data showing a) Storage modulus (E') and b) tan(δ) versus temperature for PI (black), PI SWNTs (orange) and PI-daMINT (blue).

2.4. Fabrication and characterization of carbon fiber composites PI-daMINT:

One of the main potential uses of mechanically strong PI CANs is as substitutes for thermoset epoxy resins in composites with carbon fiber (CF) mats, allowing for their reshape, repair and recycling.[26] With this in mind, we made a prototype CF-PI-daMINT composite by sandwiching a commercially available CF mat between two films of PI-daMINT (1% w/w SWNT) using a hot press (see Experimental Section for details). As a reference, we followed the same procedure to make a CF-PI composite. The CF-PI-daMINT and CF-PI films were made to have the same thickness to ensure a similar CF to polymer ratio. The mechanical characterization of the films is shown in Figure 4. In tensile tests (Figure 4a), the CF-PI composite showed a YM of 12.2 ± 0.5 GPa and a TS = 140 ± 33 MPa. We note that these values are comparable to those obtained by Zhang and co-workers for a similar composite material.[26] The reinforcement by addition of MINTs is significant, with the CF-PI-daMINT composite showing YM = 20.3 ± 0.8 GPa and a TS = 242 ± 11 MPa, that is, an improvement of 66% in YM and 73% in TS. To put these data into perspective, Burkov and Eremin studied CF-epoxy composites with carbon nanofillers extensively, and reported a maximum reinforcement of 14 % in TS by addition of 0.3% w/w SWNTs to an epoxy matrix.[27]

The DMA data of the films is shown in Figure 4b and c and confirms the reinforcement. The CF-PI film showed a storage modulus of 5.9 GPa at 25ºC while the CF-PI-daMINT film showed E'= 14.5 GPa, a 146% increase. The Tg, on the other hand, increases considerably for the CF-PI-daMINT (109 ºC) compared to the CF-PI composite (85ºC).

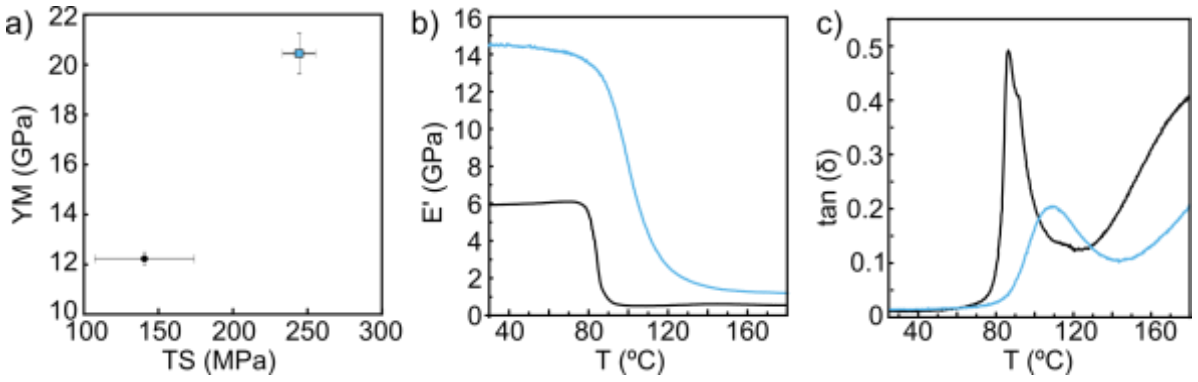

Figure 4. a) YM vs TS plot for the data obtained from the average of three stress-strain curves recorded for CF-PI (black circle) and CF-PI-daMINTs (blue square), the error bars represent the standard deviation. DMA data showing b) Storage modulus (E') and c) tan(δ) versus temperature for CF-PI (black) and CF-PI-daMINT (blue).

3. Conclusion

In conclusion, we reveal that daMINTs can be used to reinforce PI CANs with close to optimal efficiency, and that the PI-daMINT materials are recyclable by both melting and reprocessing and by chemical depolymerization and repolymerization. A key feature is the decoration of the daMINT macrocycle with a diamino group capable of participating in the imine exchange. This ensures both better dispersion of the SWNTs and enhanced load transfer, as matrix and MINT filler are directly linked through the mechanical bonds. For comparison, the composites made with pristine SWNTs showed very little reinforcement at the same SWNT loading, while the ctrlMINT bearing no diamino groups showed a meaningful but suboptimal reinforcement. Besides the mechanical data, the enhancement in load transfer from the PI matrix to the SWNT material is clearly shown in Raman spectroscopy and SEM.

We also show that the PI-daMINT material provides superior mechanical properties to single ply CF composites, compared to neat PI. The improvement in both YM and TS are very large (ca. 70%) at 1% w/w SWNT loading, as demonstrated by both tensile tests and DMA measurements.

From a more general point of view, we demonstrate that MINTs are attractive SWNT derivatives to reinforce recyclable polymers. In particular, we believe the covalent linkage of the macrocycles to the polymer matrix is the best approach to fully benefit from the outstanding mechanical properties of the SWNTs. This type of composites would have a doubly beneficial effect on the environment, as it would reduce the initial wear of the composite (due to improved mechanical properties) and allow for easy recycling (unlike thermoset plastics).

4. Experimental Section

Experimental procedure: daMINT- Polyimine composite:

Polyimine film was synthesized from a mixture of terephthaldehyde (TPA), diethylene triamine (DETA) and tris(2-aminoethyl)amine (TREN) at a molar ratio of 1.00 : 0.30: 0.47.

TPA (1 g, 7.45mmol) and daMINTs in the corresponding weight of SWNTs to create 1% wt. and 5% wt. composites were added to a 20 mL ball mill reactor and milled for 10 minutes at 250 rpm with 5 stainless steel balls of 10 mm. Then DETA (0.229g g, 2.21 mmol) and TREN (0.508g g, 3.47 mmol) were added drop by drop with a syringe, spreading it well through the dark gray powder obtained in the previous milling. This mixture was put back into the ball mill for 10 minutes at 250 rpm. Then, the ball mill reactor was opened and the paste generated inside the reactor was removed with a spatula, detaching it from the walls of the reactor and chopping it for better mixing. Next, it was put back into the ball mill to mix it for 20 minutes at 250 rpm. The homogeneous paste was taken out of the reactor to put it inside the hot press between Teflon films for its curing for 1 hour at 75ºC, 1 hour at 85ºC and 3 hours at 105ºC with a pressure of 80 bars.

Recycling of MINT- Polyimine films

The pieces of the films broken in the tensile tests were placed in the hot press at 130 ºC for 15 minutes with a pressure of 80 bars, obtaining a single film to be able to measure it again.

MINT- Polyimine- Carbon Fiber (CF) composite

Polyimine film was synthesized from a mixture of terephthaldehyde (TPA), diethylene triamine (DETA) and tris(2-aminoethyl)amine (TREN) at a molar ratio of 1.00 : 0.30: 0.47.

TPA (4.44 g, 33.1 mmol) and MINTs in the corresponding weight of SWNTs to create 1% wt. and 5% wt. composites were added to a 20 mL ball mill reactor and milled for 10 minutes at 250 rpm with 5 stainless steel balls of 10 mm. Then DETA (1.02 g, 9.90 mmol) and TREN (2.26 g, 15.4 mmol) were added drop by drop with a syringe, spreading it well through the dark

gray powder obtained in the previous milling. This mixture was put back into the ball mill for 10 minutes at 250 rpm. Then ball mill reactor was opened, and the paste generated inside the reactor was removed with a spatula, detaching it from the walls of the reactor and chopping it for better mixing, and it was put back into the mil ball to mix it for 20 minutes at 250 rpm.

The homogeneous paste is taken out of the reactor and divided into two equal parts as to their weight. Each of this paste-like material was hot-pressed using thin (0.2mm) square-shaped mold (70 mm x 70 mm) for 20 minutes at 75ºC, then and these semi-cured films were taken out of the mold. Using the same mold, a sheet of CF was fixed on the mold with adhesive tape and a sandwich was made with the two films obtained in the previous step, one on each side of the carbon fiber layer. The resulting material was cured for 1 hour at 75ºC, 1 hour at 85ºC and 3 hours at 105ºC in the hot press with a pressure of 80 bars.

Characterization

The mechanical tensile measurements of the films were carried out with Instron 34TM-10 universal testing machine. The measurements were made with a tensile rate of 1 mm/min and a distance between grips of 25 mm. The mechano-dynamic measurements of the samples were carried out with a TA DMA850 dynamic mechanical analyzer. These measurements were carried out with a film clamp and using the following conditions: amplitude of 1 µm, frequency of 1 Hz and heating rate of 5ºC/min. For the characterization of the reaction of the U-shape with Terephthaldehyde, a FT-IR compact alpha spectrometer was used.

SEM imaging and sample preparation

A Sigma Field Emission Scanning Electron Microscope was used to obtain images of the fracture surface of composites with SWNTs. The samples were prepared by cutting a 2-3 mm segment from the fracture zone of a dog bone specimen tested in a tensile test and attach it to the SEM holder using copper tape.

AFM imaging and sample preparation

A NTEGRA ACADEMIA instrument was used to obtain images of the MINTs. For image processing and measuring the heights of the SWNTs, the Gwyddion software was used. To prepare the samples, a solution of MINTs at 0.05 mg/mL in isopropanol was sonicated for one hour in a Nano Premixer THINKY at 400 rpm. The solution was then drop-cast onto a Mica substrate and allowed to dry for 1 hour at 100 ºC on a hot plate and overnight under vacuum in the Schlenk line.

Raman measurements and sample preparation

Raman measurements and optical images were performed using a commercial confocal Raman microscope (Senterra II, Bruker). Raman maps of variable size or individual Raman spectra were acquired using 785nm wavelength, 30 second acquisition, 2 coadquisitions, 9-15 cm^{-1} resolution using a 50X Olympus objective.

Supporting Information

Supporting Information is available from the Wiley Online Library or from the author.

Acknowledgements

This research was carried out with funding from Nanocore ApS (Copenhagen, Denmark). The authors would also like to acknowledge funding from the Ministerio de Ciencia e Innovación (PID2020-116661RB-I00) and the Comunidad de Madrid (MAD2D-CM)-IMDEA project funded by Comunidad de Madrid, by the Recovery, Transformation and Resilience Plan, and by NextGenerationEU from the European Union. IMDEA Nanociencia receives support from the “Severo Ochoa” Programme for Centres of Excellence in R&D (MICINN, Grant CEX2020-001039-S).

Received: ((will be filled in by the editorial staff))

Revised: ((will be filled in by the editorial staff))

Published online: ((will be filled in by the editorial staff))

References

[1] a) Y. Chen, A. K. Awasthi, F. Wei, Q. Tan, J. Li, *Science of the total environment* **2021**, *752*, 141772; b) E. J. North, R. U. Halden, *Reviews on environmental health* **2013**, *28*, 1-8.

[2] T. R. Walker, *Current Opinion in Green and Sustainable Chemistry* **2021**, *30*, 100497.

[3] a) T. Thiounn, R. C. Smith, *Journal of Polymer Science* **2020**, *58*, 1347-1364; b) J. Hopewell, R. Dvorak, E. Kosior, *Philosophical Transactions of the Royal Society B: Biological Sciences* **2009**, *364*, 2115-2126.

[4] a) P. Jagadeesh, S. Mavinkere Rangappa, S. Siengchin, M. Puttegowda, S. M. K. Thiagamani, M. Hemath Kumar, O. P. Oladijo, V. Fiore, M. M. Moure Cuadrado, *Polymer Composites* **2022**, *43*, 5831-5862.

[5] a) L. Jiang, Y. Zhou, F. Jin, *Polymer Composites* **2022**, *43*, 4835-4847; b) S.-S. Yao, F.-L. Jin, K. Y. Rhee, D. Hui, S.-J. Park, *Composites Part B: Engineering* **2018**, *142*, 241-250.

[6] a) V. Zhang, B. Kang, J. V. Accardo, J. A. Kalow, *Journal of the American Chemical Society* **2022**, *144*, 22358-22377; b) M. Podgórski, B. D. Fairbanks, B. E. Kirkpatrick, M. McBride, A. Martinez, A. Dobson, N. J. Bongiardina, C. N. Bowman, *Advanced Materials* **2020**, *32*, 1906876; c) C. J. Kloxin, C. N. Bowman, *Chemical Society Reviews* **2013**, *42*, 7161-7173.

[7] a) J. Rowan Stuart, J. Cantrill Stuart, R. L. Cousins Graham, K. M. Sanders Jeremy, J. F. Stoddart, *Angewandte Chemie* **2002**, *41*, 898-952.; b) C. Bowman, F. Du Prez, J. Kalow, *Polymer Chemistry* **2020**, *11*, 5295-5296.

[8] Z. Zhang, D. Lei, C. Zhang, Z. Wang, Y. Jin, W. Zhang, X. Liu, J. Sun, *Advanced Materials* **2023**, *35*, 2208619.

[9] C. Cui, F. Wang, X. Chen, T. Xu, Z. Li, K. Chen, Y. Guo, Y. Cheng, Z. Ge, Y. Zhang, *Advanced Functional Materials* **2024**, *n/a*, 2315469.

[10] K. I. Tserpes, P. Papanikos, *Composites Part B: Engineering* **2005**, *36*, 468-477.

[11] J. P. Salvetat, J. M. Bonard, N. H. Thomson, A. J. Kulik, L. Forró, W. Benoit, L. Zuppiroli, *Applied Physics A* **1999**, *69*, 255-260.

[12] a) J. Chen, L. Yan, W. Song, D. Xu, *Composites Part A: Applied Science and Manufacturing* **2018**, *114*, 149-169; b) Z. Spitalsky, D. Tasis, K. Papagelis, C. Galiotis, *Prog. Polym. Sci.* **2010**, *35*, 357-401; c) M. Moniruzzaman, K. I. Winey, *Macromolecules* **2006**, *39*, 5194-5205; d) J. N. Coleman, U. Khan, W. J. Blau, Y. K. Gun'ko, *Carbon* **2006**, *44*, 1624-1652; e) R. Andrews, M. C. Weisenberger, *Current Opinion in Solid State and Materials Science* **2004**, *8*, 31-37; f) I. A. Kinloch, J. Suhr, J. Lou, R. J. Young, P. M. Ajayan, *Science* **2018**, *362*, 547-553.

[13] a) X. Li, H. Ouyang, S. Sun, J. Wang, G. Fei, H. Xia, *ACS Applied Polymer Materials* **2023**, *5*, 2944-2955; b) C. Cui, L. An, Z. Zhang, M. Ji, K. Chen, Y. Yang, Q. Su, F. Wang, Y. Cheng, Y. Zhang, *Advanced Functional Materials* **2022**, *32*, 2203720.

[14] D.-M. Xie, Y.-D. Li, J.-B. Zeng, *Journal of Polymer Science* **2024**, *62*, 880-890.

[15] a) A. de Juan, Y. Pouillon, L. Ruiz-Gonzalez, A. Torres-Pardo, S. Casado, N. Martin, A. Rubio, E. M. Perez, *Angew. Chem., Int. Ed.* **2014**, *53*, 5394-5400; b) E. M. Perez,

Chem. - Eur. J. **2017**, *23*, 12681-12689; c) A. López-Moreno, S. Ibáñez, S. Moreno-Da Silva, L. Ruiz-González, N. Martín Sabanés, E. Peris, E. M. Pérez, *Angewandte Chemie International Edition* **2022**, *61*, e202208189.

[16] a) K. Miki, K. Saiki, T. Umeyama, J. Baek, T. Noda, H. Imahori, Y. Sato, K. Suenaga, K. Ohe, *Small* **2018**, 1800720; b) B. Balakrishna, A. Menon, K. Cao, S. Gsänger, S. B. Beil, J. Villalva, O. Shyshov, O. Martin, A. Hirsch, B. Meyer, U. Kaiser, D. M. Guldi, M. von Delius, *Angewandte Chemie International Edition* **2020**, *59*, 18774-18785; c) G. Cheng, T. Hayashi, Y. Miyake, T. Sato, H. Tabata, M. Katayama, N. Komatsu, *ACS Nano* **2022,** *16*, 12500.

[17] A. López-Moreno, J. Villalva, E. M. Pérez, *Chemical Society Reviews* **2022**, *51*, 9433-9444.

[18] A. López-Moreno, B. Nieto-Ortega, M. Moffa, A. de Juan, M. M. Bernal, J. P. Fernández-Blázquez, J. J. Vilatela, D. Pisignano, E. M. Pérez, *ACS Nano* **2016**, *10*, 8012-8018.

[19] S. Mena-Hernando, M. Eaton, J. P. Fernández-Blázquez, A. López-Moreno, H. Pedersen, E. M. Pérez, *Chemistry – A European Journal* **2023**, *29*, e202301490.

[20] J. Villalva, A. Rapakousiou, M. A. Monclús, J. P. Fernández Blázquez, J. de la Vega, A. Naranjo, M. Vera-Hidalgo, M. L. Ruiz-González, H. Pedersen, E. M. Pérez, *ACS Nano* **2023,** *17*, 16565.

[21] a) Villalva, J.; Pedersen, H.; López-Moreno, A.; González, M.; Pérez, E. M.; González-Juárez, M. L.; Rivas-Caramés, M.; Eaton, M. D.; Isasti, I.; Miranda, S.; Lundorf, M. D.; Naranjo-Chacón, A. Composite materials and processes for the preparation thereof. EP22382606.6, 2022; b) González-Sánchez, M.; Pedersen, H.; López-Moreno, A.; Villalva, J.; Eaton, M. D.; González-Juárez, M. L.; Pérez, E. M.; Isasti, I.; Miranda-Alcázar, S.; Rivas-Caramés, M.; Naranjo-Chacón, A.; Lundorf, M. D. Repairable and conductive nanocomposites, in situ polymerization and mechanochemistry. EP23382038.0, 2022. c) Rapakousiou, A.; Pérez, E. M.; Pedersen, H.; Lundorf, M. D.; Villalva, J. Ring-opening metathesis reactions for preparation of carbon nanotube composites. PCT/EP2022/067741, 2021. d) Pedersen, H.; González, M.; López-Moreno, A.; Villalva, J.; Gonzalez-Juarez, M. L.; Eaton, M. D.; Perez, E. M.; Lundorf, M. D.; Isasti, I.; Miranda-Alcazar, S.; Rivas-Carames, M.; Naranjo, A.; Zhang, W.; Xu, W.; Mena-Hernando, S. Industrial use of the Lasso principle for carbon nanotube composite production. PCT/EP2022/067728, 2021. e) Mena-Hernando, S.; Pérez, E. M.; Xu, W.; Zhang, W.; Pedersen, H.; Lundorf, M. D.; López-Moreno, A. Electrospinning of carbon nanotube composites. PCT/EP2022/067756, 2021. f) Pedersen, H.; Lundorf, M. D.; Dehli, T.; Nielsen, C. B. O. Composite Materials Comprising Mechanical Ligands. EP3737711, 2018. g) Lundorf, M.; Pedersen, H.; Dehli, T. Design of composite materials with desired characteristics. US11028240, 2015.

[22] X. He, X. Shi, C. Chung, Z. Lei, W. Zhang, K. Yu, *Composites Part B: Engineering* **2021**, *221*, 109004.

[23] P. Yu, H. Wang, T. Li, G. Wang, Z. Jia, X. Dong, Y. Xu, Q. Ma, D. Zhang, H. Ding, B. Yu, *Advanced Science* **2023**, *10*, 2300958.

[24] J. Du, J. Bai, H. Cheng, *Express Polymer Letters* **2007**, *1*, 253-273.

[25] D. G. Papageorgiou, Z. Li, M. Liu, I. A. Kinloch, R. J. Young, *Nanoscale* **2020**, 12, 2228.

[26] P. Taynton, H. Ni, C. Zhu, K. Yu, S. Loob, Y. Jin, H. J. Qi, W. Zhang, *Advanced Materials* **2016**, 28, 2904.

[27] M. V. Burkov, A. V. Eremin, *Polymer Composites* **2021**, 42, 4265